Thermal Properties and Morphology of Recycled Poly(ethylene terephthalate)/Maleic Anhydride Grafted Linear Low-Density Polyethylene Blends

Hongsheng Zhang, Yue Zhang, Weihong Guo, Dongdong Xu, Chifei Wu

Polymer Alloy Laboratory, School of Materials Science and Engineering, East China University of Science and Technology, 130 Meilong Road Shanghai 200237 People's Republic of China

Received 13 November 2007; accepted 18 March 2008
DOI 10.1002/app.28456
Published online 2 June 2008 in Wiley InterScience (www.interscience.wiley.com).

ABSTRACT: Properties of recycled Poly(ethylene terephthalate) were greatly improved. Recycled PET was blended with LLDPE-*g*-MA by low-temperature solid-state extrusion. Mechanical properties of the blends were affected obviously by the added LLDPE-*g*-MA. Elongation at break reaches 352.8% when the blend contains 10 wt % LLDPE-*g*-MA. Crystallization behavior of PET phase was affected by LLDPE-*g*-MA content. Crystallinity of PET decreased with the increase of LLDPE-*g*-MA content. FTIR testified that maleic anhydride group in LLDPE-*g*-MA reacted with the end hydroxyl groups of PET and PET-*co*-LLDPE-*g*-MA copolymers were *in situ* synthesized. SEM micrographs display that LLDPE-*g*-MA phase and PET phase are incompatible and the compatibility of the blends can be improved by the forming of PET-*co*-LLDPE-*g*-MA copolymer. LLDPE-*g*-MA content was less, the LLDPE-*g*-MA phase dispersed in PET matrix fine. With the increase of LLDPE-*g*-MA content, the morphology of dispersed LLDPE-*g*-MA phase changed from spherule to cigar bar, then to irregular spherule. © 2008 Wiley Periodicals, Inc. J Appl Polym Sci 109: 3546–3553, 2008

Key words: recycled poly(ethylene terephthalate); maleic anhydride grafted linear low-density polyethylene; low-temperature solid-state extrusion; mechanical properties

INTRODUCTION

Poly(ethylene terephthalate) (PET), a low cost and high performance thermoplastics, is widely used as packaging materials, fiber, and sheet due to good rigidity, hardness, abrasion resistance, solvent resistance, and electric insulation. But the strong notch sensitivity of PET restricts it from being used as engineering thermoplastics. Compared with all kinds of consumed plastics, it is easier for recycled PET beverage bottles to be separated and purified, which makes it possible to develop new applications of recycled PET. In all recycling methods, mechanical technology, including manufacturing PET blends or alloys, is a relatively simple and straightforward approach.[1–3]

Many researches have reported that the blending of PET with polyolefins and/or elastomers can improve the mechanical properties of PET.[4–16] The effect of SEBS-*g*-MA on properties of PET was extensively investigated by Atnrattanakul[4,5] and Yu.[6] Among hundreds of papers that have been published on the area of polyester/polyolefin blends, few papers focused on maleic anhydride grafted linear low-density polyethylene (LLDPE-*g*-MA) modifying PET. Linear low-density polyethylene (LLDPE) is one of the most important commercial polyolefins. Because of its nonpolar characteristic, it has poor compatibility and adherence with other materials, which limits its applications. Similar to styrene-ethylene/butylenes-styrene triblock copolymer (SEBS), polypropylene (PP) and polyethylene-propylene copolymer (EP),[4–16] polar monomer grafted polyolefin can be used as modifier or compatibilizer of polymer blends such as polyolefin/polyamides, polyesters etc.

In our previous work, low-temperature solid-state extrusion technology was investigated intensively, which is different from other kinds of extrusion.[17–19] The hydrolytic degradation and thermal degradation of PET result in poor mechanical properties. For recycled PET, it is difficult to maintain its mechanical properties after melt extrusion.[17–23] In this research, recycled PET was extruded at a temperature lower than cold-crystallization temperature of PET (T_c) at prezone and close to the melting temperature of PET (T_m) at die. Materials were crushed, plasticized, and blended by the shear force of screws rotating. Extrusion process was successfully conducted, and the degradation of PET was improved.[17–19]

In this research, maleic anhydride grafted linear low-density polyethylene (LLDPE-*g*-MA) was used to modify recycled PET beverage bottles by low-

Correspondence to: W. Guo (guoweihong@ecust.edu.cn).
Contract grant sponsor: National Natural Science Foundation of China; contract grant number: 20574019.

TABLE I
Compositions of the Blends

Blend samples	R-PET (w %)	LLDPE-*g*-MA (w %)	LLDPE
100/0	100	–	–
80/20	80	–	20
90/10MA	90	10	–
85/15MA	85	15	–
80/20MA	80	20	–
75/25MA	75	25	–
70/30MA	70	30	–

temperature solid-state extrusion. The effects of the LLDPE-*g*-MA content on mechanical properties, thermal properties, and morphology have been investigated systematically.

EXPERIMENTAL

Materials and processing

Recycled PET scraps were from Zijiang Bottle Ltd. (Shanghai, China) with an intrinsic viscosity of 0.71 dL/g. LLDPE-*g*-MA with 1 wt % maleic anhydride was homemade. The compositions of the blends were shown in Table I.

Scraps of PET were dried in dehumidifier for 10 h at 120°C before blended by corotating twin-screw extruder, while LLDPE-*g*-MA was dried under vacuum for 10 h at 60°C. Extrusion temperature from zone 1 to zone 4 was 100, 150, 200, and 230°C, respectively. The die temperature was 240°C. The extruded granules were dried in a dehumidifying dryer for 4 h at 120°C then injected to gain samples by injection molding at 240°C.

Characterization

The melt flow index (MFI) values were obtained at 265°C with 2.16 kg load for the blends using an Automatic Flow Rate Timer from Changchun Mechanical Properties Testing Machine Ltd (China).

Tensile properties and flexural properties were tested by WSM-20KN Mechanical Properties Testing Machine, according to Chinese Standard at 23°C. Although charpy impact strength was performed by JJ-20 Memorial Impact Tester, according to Chinese Standard at 23°C. Both testing machines were manufactured by Changchun Mechanical Properties Testing Machine Ltd (China).

Differential scanning calorimeter (DSC) was performed on NETZSCH DSC PC 200 (German). Samples were heated from 50 to 280°C in a nitrogen atmosphere, then cooled down to 50°C, the second run to 280°C at the same rate of 10°C/min. Samples were taken from the injection molded specimens. Melting temperature, T_m, was determined as corresponding to the maximum of the endothermic curve.

Fourier transform infrared ray (FTIR) spectroscopy was performed by attenuated total reflectance (ATR) technique to investigate reactive compatibilization and testify that end hydroxyl of PET has reacted with maleic anhydride group of LLDPE to synthesize PET-*co*-LLDPE-*g*-MA copolymer.

Morphology of the blends was revealed by means of a Scanning Electron Microscopy (SEM) instrument (JSM 6100). Samples were fractured in liquid nitrogen and coated with gold before testing.

RESULTS AND DISCUSSION

Melt flow index (MFI)

MFI value of *R*-PET/LLDPE blend (80/20 w/w) is 36.56 g/10 min, which is higher than that of virgin *R*-PET (32.98 g/10 min)and *R*-PET/LLDPE-*g*-MA blends, respectively. Because PET and LLDPE are incompatible, the high interfacial energy and surface tension result in poor adherence between PET phase and LLDPE phase. MFI values of *R*-PET/LLDPE-*g*-MA blends were greatly affected by LLDPE-*g*-MA content. With the increase of LLDPE-*g*-MA content, Figure 1 shows MFI values of blends decreased from 30.00 g/10 min to 23.51 g/10 min. *R*-PET/LLDPE-*g*-MA blends show lower MFI, which attributes to the reaction between anhydride group of LLDPE-*g*-MA and end hydroxyl of PET to synthesize PET-*co*-LLDPE-*g*-MA copolymer. The copolymer acts as compatilizer of PET and LLDPE-*g*-MA. The microstructure and rheology of blends were improved.

Mechanical properties

Table II lists the effect of LLDPE-*g*-MA contents on mechanical properties of blends. The addition of 10 wt % LLDPE-*g*-MA increased elongation at break

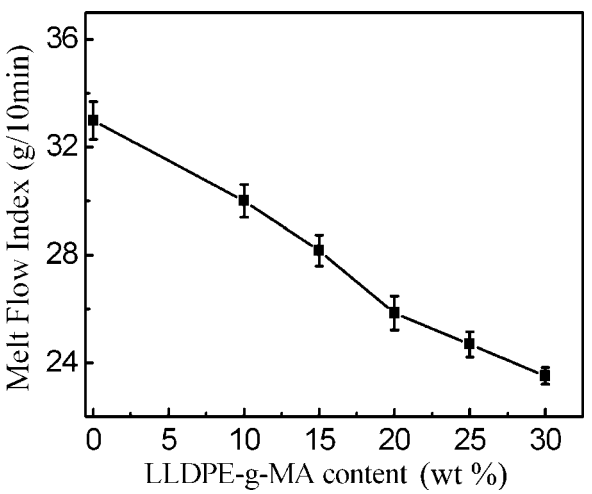

Figure 1 Effect of LLDPE-*g*-MA content on MFI of *R*-PET/LLDPE-*g*-MA blends.

TABLE II
Mechanical Properties of R-PET/LLDPE-*g*-MA Blends

Blend samples	Charpy impact strength (kJ/m^2)	Elongation at break (%)	Yield stress (MPa)	Flexural strength (MPa)	Flexural modulus (MPa)
100/0	4.73 ± 0.54	126.0 ± 26.6	55.96 ± 0.89	85.43 ± 1.66	2599.8 ± 34.2
80/20	7.3 ± 0.5	10.4 ± 4.4	35.2 ± 0.9	54.6 ± 1.6	1783.0 ± 27.6
90/10 MA	8.71 ± 0.42	352.8 ± 13.5	40.34 ± 0.69	63.59 ± 0.80	2103.6 ± 29.8
85/15 MA	9.68 ± 0.18	393.3 ± 27.8	35.94 ± 1.24	56.63 ± 1.85	1978.0 ± 48.8
80/20 MA	10.41 ± 0.50	365.2 ± 45.7	35.75 ± 2.24	52.27 ± 0.63	1675.9 ± 49.8
75/25 MA	10.33 ± 0.47	411.1 ± 13.1	32.64 ± 1.25	48.49 ± 0.50	1560.6 ± 34.9
70/30 MA	10.84 ± 0.58	414.2 ± 8.6	28.79 ± 0.43	43.14 ± 0.32	1359.5 ± 37.7

(352.8%) by 280% and decreased yield stress (40.34 MPa) by 30%, respectively. Elongation at break of blends changes slightly, while yield stress of blends decrease continuously with the increase of LLDPE-*g*-MA content. Table II also shows the charpy impact strength of the blends increases with the addition of LLDPE-*g*-MA content. At the same time, the reduction in yield stress, flexural strength and flexural modulus should be considered that strength and modulus of LLDPE-*g*-MA are lower than those of PET, the more content of LLDPE-*g*-MA, the lower mechanical properties of the blends can be gained.

LLDPE-*g*-MA can evidently improve toughness of PET in comparison to *R*-PET/LLDPE blend. PET and LLDPE are thermodynamically immiscible heterogeneous system and represent a two-phase morphology. This structure leads to poor mechanical properties.[8–13] Elongation at break of sample of *R*-PET/LLDPE blend (80/20 w/w) is only 10.4%. But for *R*-PET/LLDPE-*g*-MA blends, maleic anhydride can react with end hydroxyl group of PET to synthesize PET-*co*-LLDPE-*g*-MA copolymer, which acts as the bridge to connect PET phase with LLDPE-*g*-MA phase. Surface tension and interfacial energy between PET phase and LLDPE-*g*-MA phase are lower than those of *R*-PET/LLDPE blend. When samples were stretched in tensile testing, PET-*co*-LLDPE-*g*-MA restricted the slippage and debonding between different phases to create better ductibility. When LLDPE-*g*-MA content increased, excessive LLDPE-*g*-MA congregated in LLDPE-*g*-MA phase, the elongation at break of PET/LLDPE-*g*-MA blends will keep almost the same. Charpy impact strength of *R*-PET/LLDPE-*g*-MA blends was improved by LLDPE-*g*-MA which acts as stress transfer agent.

FTIR Spectra

PET/LLDPE-*g*-MA blend (70/30 w/w) was extracted alternately by phenol and xylene to remove unreacted *R*-PET and LLDPE-*g*-MA. Insoluble substance content is about 29 wt %. FTIR spectra of the insoluble substance, *R*-PET/LLDPE-*g*-MA blend 70/30 w/w, *R*-PET, and LLDPE-*g*-MA are shown in Figure 2. The bands at 1720, 1099, and 1251 cm^{-1} correspond to C=O stretching vibration, C—O (in gauche) stretching vibration and (C=O)—O stretching vibration of PET chain, respectively,.[24] The bands at 2921 and 2852 cm^{-1} are signed to the CH_2 stretching vibration of LLDPE chain. In [Fig. 2(b)], the FTIR spectra of insoluble substance involve all bands of the aforementioned groups, which proves that maleic anhydride group of LLDPE reacted with end hydroxyl group of PET to synthesize PET-*co*-LLDPE-*g*-MA copolymer.

Thermal analyses of *R*-PET/Lldpe-*g*-MA blends

Figure 3 displays transition peaks of PET that corresponds to the melting temperature of PET during second scanning. The plots show melting of virgin *R*-PET has a single peak, while PET phase in blends have double peaks. It means that LLDPE-*g*-MA affects crystallization behavior of PET greatly. Thermal properties of *R*-PET and *R*-PET/LLDPE-*g*-MA blends are listed in Table III. Table III shows melt temperature of PET is close to that of virgin *R*-PET, and crystallinities of PET phase in blends are higher

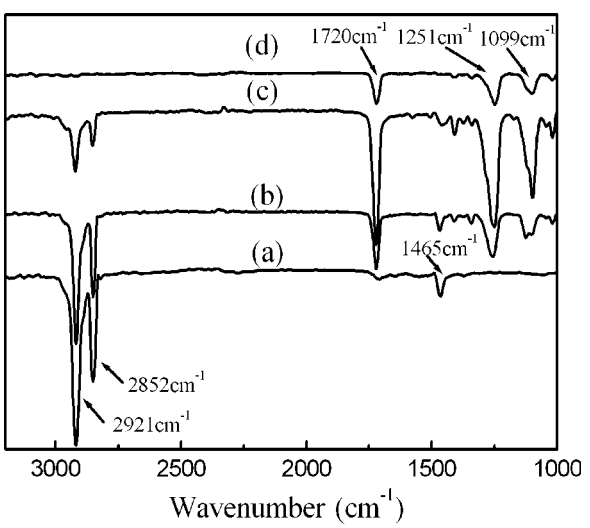

Figure 2 FTIR Spectra of (a) LLDPE-*g*-MA, (b) insoluble substance of PET/LLDPE-*g*-MA blend (70/30 w/w) extracted alternately by phenol and xylene, (c) *R*-PET/LLDPE-*g*-MA blend (70/30 w/w), (d) *R*-PET.

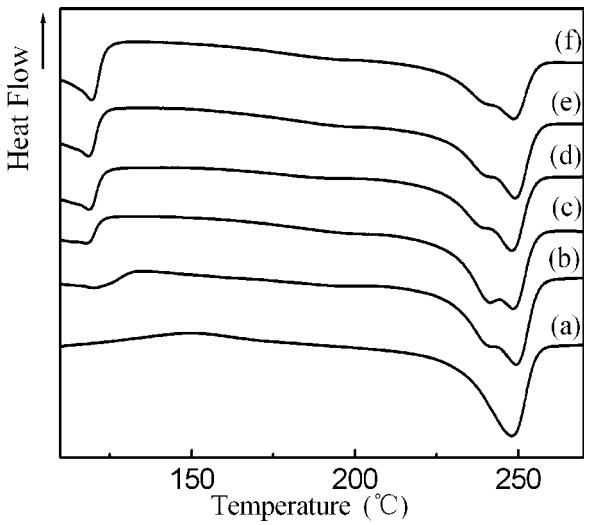

Figure 3 DSC plot of *R*-PET/LLDPE-*g*-MA blends recorded during second scanning LLDPE-*g*-MA content: (a) 0 w %, (b) 10 w %, (c) 15 w %, (d) 20 w %, (e) 25 w %, (f) 30 w %.

than that of virgin *R*-PET. The results also show that crystallinity of PET decreased with the increase of LLDPE-*g*-MA content.

It is easy for PET to degrade by thermal degradation and hydrolytic degradation to generate end hydroxyl group and carboxyl group during extrusion processing. These generated and original hydroxyl group can react with maleic anhydride group of LLDPE-*g*-MA to synthesize PET-*co*-LLDPE-*g*-MA copolymer by interface reaction during blending. The reaction mechanism between PET and LLDPE-*g*-MA is displayed in Figure 4.

TABLE III
Summary of Thermal Properties of *R*-PET and *R*-PET/ LLDPE-*g*-MA Blends

Sample	T_m (°C)	ΔH_m (J/g)	Crystallinity (%)
100/0	247.9	−30.45	21.75
90/10 MA	249.4	−37.88	27.06
85/15 MA	248.5	−36.51	26.08
80/20 MA	248.0	−35.90	25.64
75/25 MA	249.0	−33.11	23.65
70/30 MA	248.3	−31.03	22.17

Crystallization behavior of PET is determined by two competing factors. First, one LLDPE-*g*-MA molecule which perhaps includes several maleic anhydride groups could react with several PET molecules simultaneously to produce branched PET-*co*-LLDPE-*g*-MA. It facilitates PET to congregate, orientate and form crystal cell at interface. Second, introduction of LLDPE chain into PET chain is considered as a useful method to reduce homogeneity of PET chain in copolymer that is to disadvantage of crystallization of PET. It is presumed that the two competing factors result in different crystallization behavior of PET near interface and in bulk of PET phase. Crys-

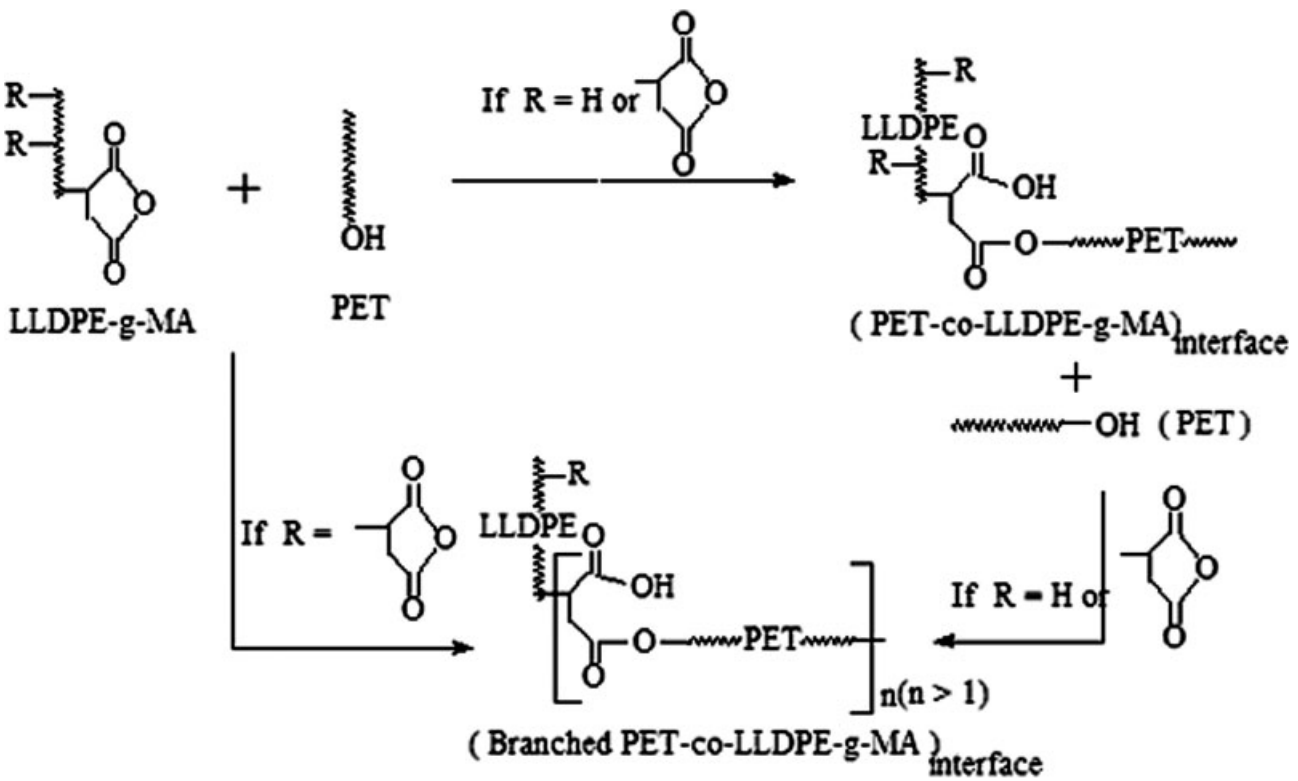

Figure 4 Proposed mechanism for *in situ* interfacial reaction that occurs during blending of PET with LLDPE-*g*-MA.

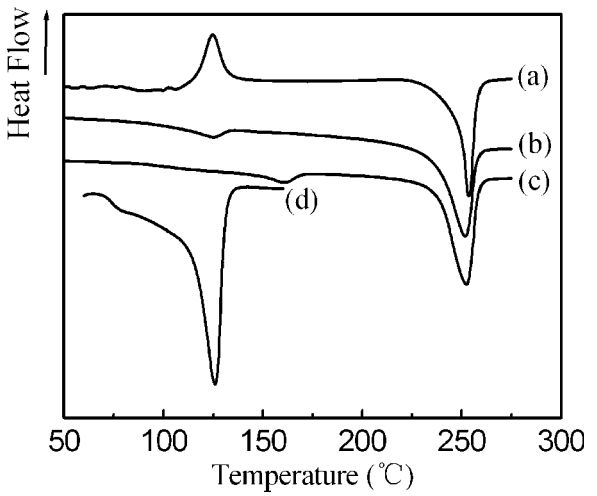

Figure 5 DSC plot of scrap of *R*-PET and LLDPE-*g*-MA (a) *R*-PET before annealed, (b) *R*-PET annealed at 130°C for 48 h, (c) *R*-PET annealed at 160°C for 72 h, (d) LLDPE-*g*-MA.

tallinity of PET in bulk phase of PET is similar to that of the virgin *R*-PET. Near interface, the crystallization behavior of PET was influenced by LLDPE-*g*-MA chain. At lower LLDPE-*g*-MA content, first factor is dominant. Most PET chains closed to interface were induced to enter into crystal cell by nucleation of PET chain of branched PET-*co*-LLDPE-*g*-MA. With the increase of LLDPE-*g*-MA content, one LLDPE-*g*-MA molecule only reacts with one PET molecule, the second factor becoming dominant. Therefore, the nucleation of PET chain of branched PET-*co*-LLDPE-*g*-MA is reduced.

Samples were annealed for further investigating the crystallization behavior of PET. The DSC plots of annealed and unannealed raw materials were displayed in Figure 5 and the thermal properties were listed in Table IV. Table IV illustrate that cold crystallization temperature of PET (124.6°C) and melting temperature of LLDPE (124.3°C) overlap mutually. It is lucky that previous literatures [19–23,25] have discussed the multiple melting behavior of PET extensively, which showed that the secondary melting temperature of PET is affected greatly by annealing temperature and time. When annealing at 130°C for 48 h, the secondary melting temperature of PET is 124.9°C (T_{sm}), which superposes melting temperature of LLDPE-*g*-MA. But when annealing at 160°C for 72 h, that of PET is 160.7°C, which is far from T_m of LLDPE-*g*-MA. Annealing temperature and time also influence the crystallization behavior of PET. In this research, samples were annealed at 160°C for 72 h has been chosen.

Figure 6 shows the effect of LLDPE-*g*-MA content on crystallization behavior of PET. Thermal properties of PET and LLDPE-*g*-MA were listed in Table V. Crystallization behavior of LLDPE-*g*-MA can be embodied by its crystallinity and melting process. In Figure 6, melting peaks of LLDPE-*g*-MA are evolved to asymmetric single peak from double peaks and melting peak of PET keeps single peak all along as the increasing of LLDPE-*g*-MA content. The LLDPE chain in PET-*co*-LLDPE-*g*-MA copolymer is less active than that in free LLDPE-*g*-MA. At low LLDPE-*g*-MA content, most LLDPE-*g*-MA can react with PET, and one LLDPE-*g*-MA molecule may react with several PET molecules. The activity of LLDPE chain can be restrained by PET chain, which results in defected crystal cell of LLDPE-*g*-MA with lower melt temperature and lower apparent crystallinity. With the increasing of LLDPE-*g*-MA content, free LLDPE-*g*-MA content in blends is increasing, and one LLDPE-*g*-MA molecule only reacts with one PET molecule, which makes it easier to form LLDPE-*g*-MA crystal cell.

Crystallization behavior of PET in annealed blends is different from that of LLDPE-*g*-MA. When LLDPE-*g*-MA content is less than 20 w %, there is no substantial effect on crystallinity of PET, but crys-

TABLE IV
Summary of Thermal Properties of *R*-PET and LLDPE-*g*-MA

	T_g (°C)	T_m (°C)	T_c (°C)	T_{sm}[a] (°C)	ΔH_m (kJ/g)	ΔH_c (kJ/g)	ΔH_{sm}[b] (kJ/g)	Crystallinity[c] (%)
R-PET	84.1	253.7	124.6	–	−32.73	15.99		11.96
R-PET[d]	–	251.9	–	124.9	−38.11		−1.63	25.79
R-PET[e]	–	252.4	–	160.7	39.79		−2.00	28.42
LLDPE-*g*-MA	–	121.0	–	–	−50.54		–	17.25

[a] Melting point of secondary crystallization.
[b] Melting enthalpy for secondary crystallization.
[c] Crystallinity, which is not including secondary crystallization, is calculated by the following equation: Crystallinity (%) $= \frac{\Delta H_m}{\Delta H_m^*} \times 100$, where ΔH_m^* = 144.664 J/g (and 293.0), is the melt enthalpy for 100% crystallized PET (and LLDPE), ΔH_m is measured major melt enthalpy for PET (and LLDPE) of blends.
[d] Annealed at 130°C for 24 h.
[e] Annealed at 160°C for 72 h.

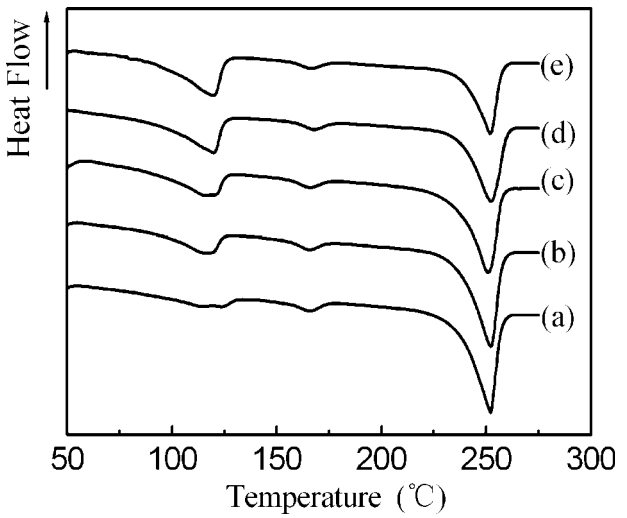

Figure 6 DSC plots of *R*-PET/LLDPE-*g*-MA blends annealed at 160°C for 72 h LLDPE-*g*-MA content: (a) 10 w %, (b) 15 w %, (c) 20 w %, (d) 25 w %, (e) 30 w %.

tallinity of PET is decreased with the increase of LLDPE-*g*-MA content. As is mentioned earlier, lower LLDPE-*g*-MA content is beneficial to forming of PET crystal cell near interface. In all samples, melting temperature of secondary crystallization (T_{sm}) is similar and higher than that of virgin *R*-PET.

Morphology

SEM micrographs of *R*-PET/LLDPE 80/20 w/w blend and *R*-PET/LLDPE-*g*-MA blends were displayed in Figure 7. As expected, *R*-PET/LLDPE blend exhibited two-phase morphology. It is clear that LLDPE formed a dispersed phase in the forming of spherical domains in the PET matrix, and most of the particles and cavities on the cryofractured surface are very smooth due to poor interface adhesion of PET phase and LLDPE phase.

The cryofactured surface of *R*-PET/LLDPE-*g*-MA blends is different from that of *R*-PET/LLDPE blend. LLDPE-*g*-MA particles dispersed in PET matrix finer, which is shown in [Fig. 7(b–d)]. Increasing LLDPE-*g*-MA content, the morphology of dispersed phase was changed from spherule to cigar bar, then to irregular spherule. Grafted copolymer (PET-*co*-LLDPE-*g*-MA) formed *in situ* act as compatibilizer for PET and LLDPE-*g*-MA, and such copolymer contribute to reducing interfacial tension and the tendency of dispersed phase to coalesce. The improved dispersion during blending processing gives rise to the reduction of average size of the dispersed phase. However, in this system, the LLDPE-*g*-MA domain size becomes larger with its content increasing. It means that PET phase and LLDPE-*g*-MA phase are imcompatible, PET-*co*-LLDPE-*g*-MA copolymer acting as compatibilizer to improve their compatibility. At lower LLDPE-*g*-MA content, dispersed phase were composed mainly of LLDPE chain of copolymer, but at higher LLDPE-*g*-MA content, unreacted LLDPE-*g*-MA and LLDPE chain of the copolymer conglomerated to form LLDPE-*g*-MA phase. Because of anisotropism of dipole–dipole interaction between LLDPE-*g*-MA phase and matrix at interface, the shape of dispersed phase of *R*-PET/LLDPE-*g*-MA 80/20 w/w blend evolved into cigar bar. When LLDPE-*g*-MA content reaches 30 w %, the shape of dispersed phase is irregular and much larger. [Fig. 7(e)] indicates that LLDPE-*g*-MA cannot be etched effectively by xylene because some smaller domains still interspersed in dispersed phase. Compared with *R*-PET/LLDPE/SEBS-*g*-MA 64/16/20 w/w/w blend,[19] many PET molecules sentered into dispersed phase to form special salami structure. So it is reasonable to consider that some PET molecules enters into LLDPE-*g*-MA phase by interface reaction during blend processing to increase dispersed phase content in this blend and affect its shape.

TABLE V
Summary of Thermal Properties of Annealed R-PET/LLDPE-*g*-MA Blends

				R-PET				
	LLDPE-*g*-MA			Crystallization			Secondary crystallization	
R-PET/LLDPE-*g*-MA	T_m (°C)	ΔH_m (J/g)	Crystallinity (%)	T_m (°C)	ΔH_m (J/g)	Crystallinity (%)	T_{sm}[a] (°C)	ΔH_{sm}[b] (J/g)
90/10 MA	108.0 122.9	−43.58	14.90	252.3	−39.41	28.15	165.8	2.46
85/15 MA	116.1	−49.48	16.89	252.3	−40.94	29.24	165.8	2.78
80/20 MA	119.5	−46.33	15.81	251.9	−41.79	29.85	165.4	3.20
75/25 MA	119.5	−49.92	17.04	251.9	−37.83	27.02	166.9	3.19
70/30 MA	119.9	−46.53	15.88	252.5	−34.00	24.28	166.9	3.03

[a] Melting point of secondary crystallization of PET.
[b] Melting enthalpy for secondary crystallization.

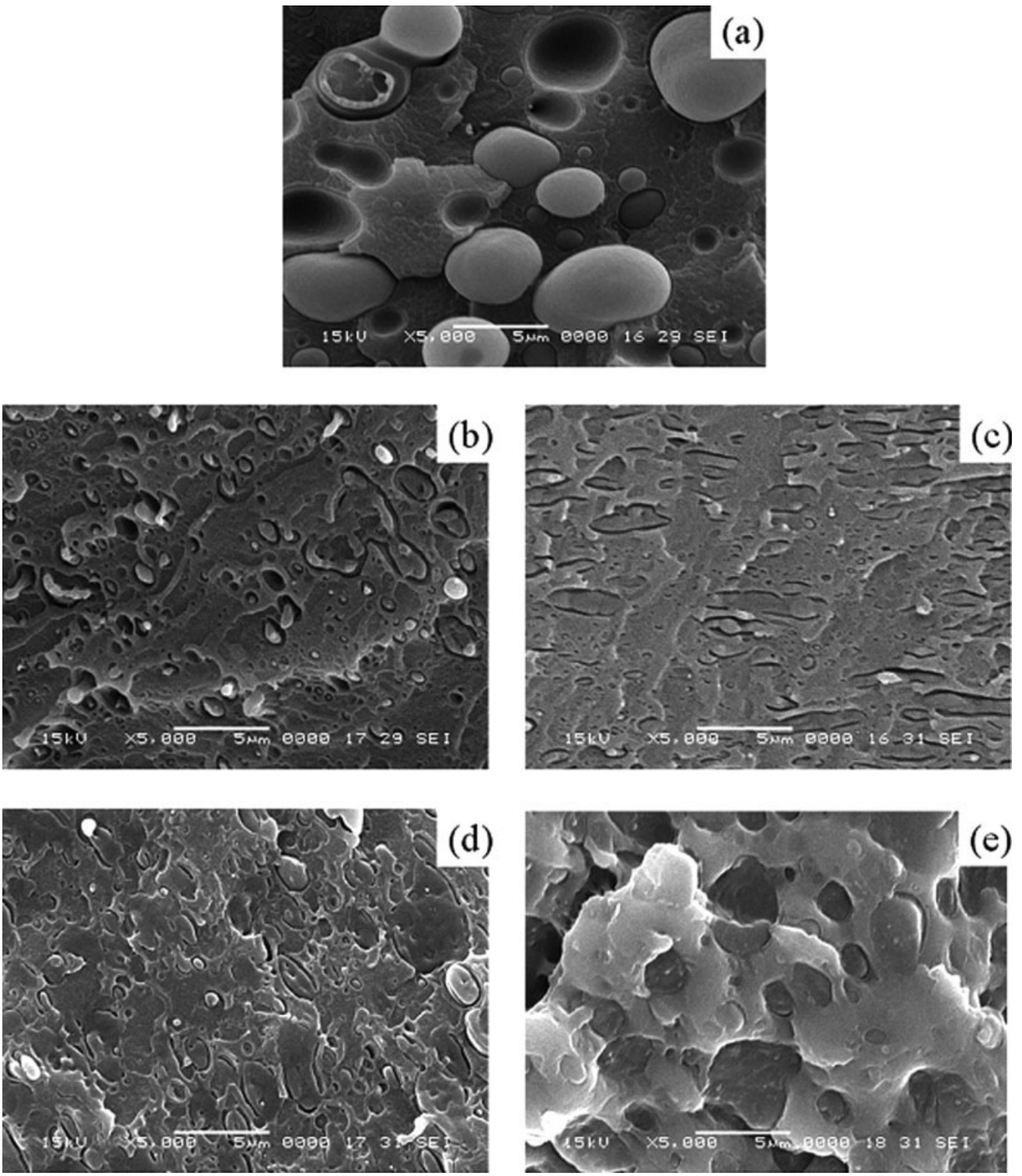

Figure 7 SEM micrograph of *R*-PET/LLDPE-*g*-MA blends (a) *R*-PET/LLDPE 80/20 w/w, (b) *R*-PET/LLDPE-*g*-MA 90/10 w/w, (c) *R*-PET/LLDPE-*g*-MA 80/20 w/w, (d) *R*-PET/LLDPE-*g*-MA 70/30 w/w, (e) *R*-PET/LLDPE-*g*-MA 70/30 w/w, etched by xylene.

CONCLUSIONS

LLDPE-*g*-MA acted as a modifier to improve rheology and mechanical properties of recycled PET. With the increase of LLDPE-*g*-MA content, MFIs of *R*-PET/LLDPE-*g*-MA blends were decreased. Elongation at break of *R*-PET/LLDPE-*g*-MA blend was increased from 162.0% to 352.8% by adding 10 w % LLDPE-*g*-MA. Adding more LLDPE-*g*-MA cannot further increase terminal elongation of *R*-PET/LLDPE-*g*-MA blends.

FTIR testifies that PET-*co*-LLDPE-*g*-MA copolymer was *in situ* synthesized and played an important role in crystallization behavior of PET.

Thermal analysis illustrates that two competing factors effected crystallization behavior of PET obviously. For unannealed *R*-PET/LLDPE-*g*-MA blends, crystallinity of PET was decreasing with the increase of LLDPE-*g*-MA content. Lower LLDPE-*g*-MA content benefits the forming of PET crystal cell. With the increasing of LLDPE-*g*-MA content, PET-*co*-LLDPE-*g*-MA copolymer destroys regular structure of PET chain, which restricts PET chain entering into crystal cell and decreased the crystallinity of PET. However, when LLDPE content is less than 20 w %, there is some influence on the secondary melt temperature of PET but not obviously on the crystallinity of PET.

The effect of LLDPE-*g*-MA content on microstructure of PET/LLDPE-*g*-MA blends was also investigated by SEM. Dispersed phase dispersed fine in PET matrix when LLDPE-*g*-MA content is less than 20 w %. Because of incompatibility, the morphology of dispersed phase changed with the increase of LLDPE-*g*-MA content from spherule to cigar bar, then to spherule. The improvement of mechanical thermal properties of *R*-PET proved that PET-*co*-LLDPE-*g*-MA copolymer increased the compatibility of the blends.

References

1. Pracella, M.; Rolla, L.; Chionna D.; Galeski A. Macromol Chem Phys 2002, 203, 1473.
2. Ávila, A. F.; Duarte, M. V. Polym Degrad Stab 2003, 80, 373.
3. Scott, G. Polym Degrad Stab 2000, 68, 1.
4. Tanrattanakul, M. W.; Hiltner, A.; Baer, E.; Perkins, W. G.; Massey, F. L.; Moet, A. Polymer 1997, 38, 2191.
5. Tanrattanakul, M. W.; Hiltner, A.; Baer, E.; Perkins, W. G.; Massey, F. L.; Moet, A. Polymer 1997, 38, 4117.
6. Yu, Z. Z.; Yang, M. S.; Dai, S. C.; Mai, Y. W. J Appl Polym Sci 2004, 93, 1462.
7. Mouzakis, D. E.; Papke, N.; Wu, J. S.; Karger-Kocsis, J. J Appl Polym Sci 2001, 79, 842.
8. Chem, L. E.; Woong, B.; Baker, W. E. Polym Eng Sci 1996, 36, 1594.
9. Bidoux, J. E.; Smith, G. D.; Bernet, N.; Manson, J. A. E.; Hilborn, J. Polymer 1996, 37, 1129.
10. Saleem, M.; Baker, W. E. J Appl Polym Sci 1990, 39, 655.
11. Pluta, M.; Bartczak, Z.; Pawlak, A.; Galeski, A.; Pracella, M. J Appl Polym Sci 2001, 82, 1423.
12. Retolaza, A.; Eguiazábal, J. I.; Nazábal, J. J Appl Polym Sci 2003, 87, 1322.
13. Shi, T. F.; Ziegler, V. E.; Welge, I. C.; et al. Mocromolecules 2004, 37, 1591.
14. Kim, J. K.; Kim, S.; Park, C. E. Polymer 1997, 38, 2155.
15. Yong, M. W.; Xanthos, M.; Biesenberger, J. A. Polym Eng Sci 1990, 30, 355.
16. Parlak, A.; Perkins, W.; Perkins, W. G.; Baer, E. J Appl Polym Sci 1999, 73, 203.
17. Guo, W. H.; Tang, X. W.; Yin, G. R.; et al. J Appl Polym Sci 2006, 102, 2692.
18. Tang, X. W.; Guo, W. H.; Yin, G. R.; et al. Polym Bull, Published online.
19. Zhang, H. S.; Yu, Y. B.; Guo, W. H.; Li, B. Y.; Wu, C. F. Eur Polym J 2000, 43, 3662.
20. Holdsworth, P. J.; Turner-Jones, A. Polymer 1995, 28, 2845.
21. Alfonso, G. C.; Pedemonte, E.; Ponzetti, L. Polymer 1979, 20, 104.
22. Rpberts, R. C. Polymer 1969, 10, 117.
23. Chen, H.-L. Macromolecules 1995, 28, 2845.
24. Wang, Y.; Shen, D. Y.; Qian, R. Y. J Polym Sci Part B: Polym Phy 1998, 36, 783.
25. Chen, H.-L. Polymer 1996, 27, 5461.